2010 IEEE/ASME International Conference on
Advanced Intelligent Mechatronics
Montréal, Canada, July 6-9, 2010

Contouring Control of Biaxial Systems Based on a New Task Coordinate Frame

Chuxiong Hu, Bin Yao, and Qingfeng Wang

Abstract— **This paper proposes a new task coordinate frame (TCF) for contouring control of biaxial systems. Existing task coordinate frames are only locally defined based on the desired contouring trajectory to be tracked and the calculated contour error is an approximation to the actual contour error only. As such, they are applicable to contouring tasks with small curvature and little actual trajectory tracking errors only. In contrast, the proposed task coordinate frame is globally defined based on the geometry of the desired contour only and the resulting coordinate errors correspond to the actual contouring error and the tangential error on the contour directly. To demonstrate the high contouring performance nature of the proposed task coordinate frame, the system dynamics of a biaxial linear motor gantry is transformed into this task coordinate frame. A discontinuous projection based adaptive robust controller (ARC) which explicitly takes into account the dynamic coupling effect is then employed to improve the contouring performance under both parametric uncertainties and uncertain nonlinearities. Comparative experimental results obtained on a high-speed industrial biaxial gantry driven by linear motors are presented to verify that the proposed TCF is effective for achieving excellent contouring performance even when large-curvature contouring control tasks are of concern.**

I. Introduction

Contour-following is one of the most ubiquitous motion control problems encountered by servomechanisms such as integrated circuit (IC) manufacturing equipments, robot manipulators, and computer numerical control (CNC) machine tools. Earlier researches on the coordinated contouring control [1]–[7] use the cross-coupled control (CCC) strategy first proposed by Koren [8], in which coupling actions was introduced in the servo controllers to strengthen the motion coordination of multi-axes. However, the proposed representations of contouring errors are approximate and effective only for applications with small curvature path. In addition, the presented algorithms were based on the traditional control theories for linear time-invariant systems and cannot address the dynamic coupling phenomena (e.g. Coriolis force) well when tracking curved contours. Chiu and Tomizuka [9] formulated the contouring control problem into a task coordinate frame "attached" to the desired contour. Under the task coordinate formulation, a control law could be designed to assign different dynamics to the normal and tangential directions relative to the desired contour. Since then many contouring control schemes based on task coordinate approaches have been reported [10]–[14]. However, the task coordinate frames used in all these work are locally defined based on the desired trajectory to be tracked on the desired contour, which is valid only for applications with very small actual tracking errors and small curvatures. They would not be sufficient when large curvature contouring is of main concern or significant tracking errors exhibit due to sudden disturbances.

In this paper, as opposed to approximate estimations of contouring errors [5], [7], [10], a new task coordinate frame will be developed based on the geometry of the desired contour only. Such a task coordinate frame (TCF) is globally defined and has nothing to do with the specific desired trajectory to be tracked on the contour. The calculated contouring error is directly related to the actual contouring error and not affected by the curvature of the desired contour. To test the effectiveness of the proposed TCF, the system dynamics of a biaxial linear motor gantry is transformed into this task coordinate frame, and a discontinuous projection based adaptive robust controller (ARC) [16], [17] which explicitly takes into account the dynamic coupling effect is then employed to improve the contouring performance under both parametric uncertainties and uncertain nonlinearities. For comparison, the traditional TCF [11]–[14] and the proposed TCF with the same ARC controller are both implemented on a high-speed industrial biaxial gantry driven by LC-50-200 linear motors with a linear encoder resolution of 0.5 μm. Comparative experimental results obtained on the biaxial gantry demonstrate that the proposed algorithm is able to achieve excellent contouring performance even when the tasks of high-speed and large-curvature contouring are required.

II. Problem Formulation

A. Task Coordinate Frame

We will approach the definition of the task coordinate frame from a new perspective as follows. Traditionally, the task coordinate frame for a biaxial system is locally defined at the desired position $P_d(x_d(t), y_d(t))$ based on the desired trajectory on the desired contour given by

$$\mathbf{q_d}(t) = [x_d(t), y_d(t)]^T \tag{1}$$

Such a definition depend on not only the geometry of the desired contour (e.g., a circle or an ellipsoidal) but also

The work is supported in part by the US National Science Foundation (Grant No. CMS-0600516), in part by the National Natural Science Foundation of China (NSFC) (Grant No. 50875233), and in part by the NSFC for Young Scholars (No. 50905158).

Chuxiong Hu, a PhD candidate, and Qingfeng Wang, a professor, are with the State Key Laboratory of Fluid Power Transmission and Control, Zhejiang University, Hangzhou, China. Their emails are fyfox.hu@gmail.com and qfwang@zju.edu.cn

Bin Yao is a Professor of School of Mechanical Engineering at Purdue University, West Lafayette, IN 47907, USA (byao@purdue.edu). He is also a Chang Jiang Chair Professor at the State Key Laboratory of Fluid Power Transmission and Control of Zhejiang University.

the desired motion to be tracked on the contour (e.g., the parametrization of the desired trajectory by the time t). As such, when the actual tracking error is large or the actual position differs from the desired point $\mathbf{q_d}(t)$ significantly, the calculated contour error could be far different from the actual one as illustrated in Fig.1 by the coordinate frame in yellow color. Intuitively, the actual contour error depends on the geometry of the desired contour and the actual path of the system only and should have nothing to do with the desired trajectory to be tracked on the contour, which is affected by other factors such as the speed of the desired motion on the contour as well. To overcome this problem, in the following, a new task coordinate from will be introduced solely on the geometry of the desired contour, which represents a single constraint in the X-Y plane and can be defined by

$$f(x,y)=0 \tag{2}$$

where x and y denote the coordinates of the biaxial gantry system in the X-Y plane and f is a known smooth shape function as shown in Fig.1. With the desired contour geometry described by Eq. (2), a curvilinear coordinate along the normal direction of the desired contour can be defined as

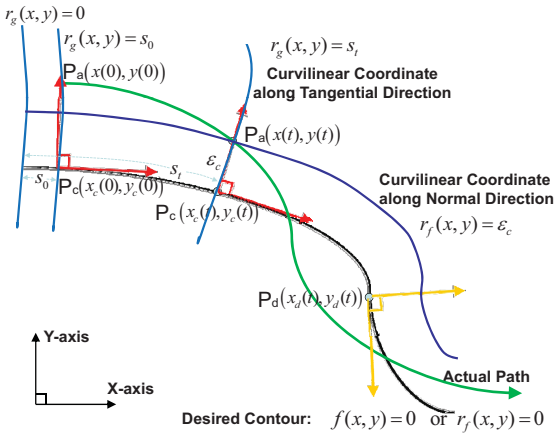

Fig. 1. A Global Task Task Coordinate Frame

$$r_f(x,y)=\frac{f(x,y)}{\sqrt{{f_x}^2+{f_y}^2}} \tag{3}$$

where $f_x=df/dx$ and $f_y=df/dy$. With this curvilinear coordinate, the desired contour can be simply described by constraining it to zero in the new task coordinate frame, i.e., $r_f(x,y)=0$, and the normal direction of the desired contour is align with the direction of this curvilinear coordinate. Furthermore, it can be shown that the coordinate value of the actual position along this curvilinear coordinate direction [1] is the same as the actual contouring error ε_c, the distance between the actual position $P_a(x(t),y(t))$ and $P_c(x_c(t),y_c(t))$, the projection of $P_a(x(t),y(t))$ onto the desired contour along its normal direction as illustrated in Fig.1.

[1] i.e., $r_f(x(t),y(t))$ where $(x(t),y(t))$ represents the Cartesian coordinates of the actual position at time t

With the above definition of the curvilinear coordinate representing the contour error, the other curvilinear coordinate $r_g(x,y)$ will be defined based on the curve length on the desired contour between the reference point and the projection of the position (x,y) at the desired contour along its normal direction, e.g., the curve lengths s_0 and s_t shown in Fig.1 for the initial position $P_a(x(0),y(0))$ and the actual position $P_a(x(t),y(t))$ respectively. Overall, the proposed task coordinate system is defined by the following curvilinear coordinate transformation:

$$\mathbf{r}=\mathbf{h}(\mathbf{q})=\begin{bmatrix} r_f(x,y) \\ r_g(x,y) \end{bmatrix} \tag{4}$$

It can be checked that, on the desired contour, the directional vector along first curvilinear coordinate r_f, $[\frac{\partial r_f}{\partial x},\frac{\partial r_f}{\partial y}]^T$, is the same as the unit vector along the normal direction of the desired contour, $[\frac{f_x}{\sqrt{f_x^2+f_y^2}},\frac{f_y}{\sqrt{f_x^2+f_y^2}}]^T$, and the directional vector along the second curvilinear coordinate r_g, $[\frac{\partial r_g}{\partial x},\frac{\partial r_g}{\partial y}]^T$, is the same as the unit vector along the tangential direction of the desired contour, $[-\frac{f_y}{\sqrt{f_x^2+f_y^2}},\frac{f_x}{\sqrt{f_x^2+f_y^2}}]^T$. It is thus obvious that, in the new task coordinate frame, the original contour tracking problem is decoupled into a regulation problem along the curvilinear coordinate r_f and a trajectory tracking problem along the curvilinear coordinate r_g. Furthermore, around the desired contour, the Jacobian matrix of the curvilinear coordinate transformation (4) can be approximated by

$$\mathbf{J}=\begin{bmatrix} \frac{\partial r_f}{\partial x} & \frac{\partial r_f}{\partial y} \\ \frac{\partial r_g}{\partial x} & \frac{\partial r_g}{\partial y} \end{bmatrix} \approx \begin{bmatrix} \frac{f_x}{\sqrt{f_x^2+f_y^2}} & \frac{f_y}{\sqrt{f_x^2+f_y^2}} \\ -\frac{f_y}{\sqrt{f_x^2+f_y^2}} & \frac{f_x}{\sqrt{f_x^2+f_y^2}} \end{bmatrix} \tag{5}$$

which is symmetric and unitary, i.e., $\mathbf{J^T}=\mathbf{J}$ and $\mathbf{J^{-1}}=\mathbf{J}$.

B. System Dynamics

The biaxial linear motor driven gantry is assumed to have the following dynamics:

$$\mathbf{M}\ddot{\mathbf{q}}+\mathbf{B}\dot{\mathbf{q}}+\mathbf{F}(\dot{\mathbf{q}})=\mathbf{u}+\mathbf{d} \tag{6}$$

where $\mathbf{q}=[x(t),y(t)]^T$, $\dot{\mathbf{q}}=[\dot{x}(t),\dot{y}(t)]^T$ and $\ddot{\mathbf{q}}=[\ddot{x}(t),\ddot{y}(t)]^T$ are the 2×1 vectors of the axis position, velocity and acceleration, respectively; $\mathbf{u}$ is the 2×1 vector of control input, and $\mathbf{d}$ is the 2×1 vector of unknown nonlinear functions due to external disturbances or modeling errors such as the force ripple; $\mathbf{M}=diag[M_1,M_2]$ and $\mathbf{B}=diag[B_1,B_2]$ are the 2×2 diagonal inertia and damping matrices, respectively; $\mathbf{F}(\dot{\mathbf{q}})$ is the 2×1 vector of nonlinear friction, and the model used in this paper is given by $\bar{\mathbf{F}}(\dot{\mathbf{q}})=\mathbf{AS_f}(\dot{\mathbf{q}})$, where $\mathbf{A}=diag[A_1,A_2]$ is the 2×2 diagonal friction coefficient matrix, and $\mathbf{S_f}(\cdot)$ is a vector-valued smooth function, i.e., $\mathbf{S_f}(\dot{\mathbf{q}})=[S_f(\dot{x}),S_f(\dot{y})]^T$. Define the approximation error as $\widetilde{\mathbf{F}}=\bar{\mathbf{F}}-\mathbf{F}$. Then equation (6) can be written as

$$\mathbf{M}\ddot{\mathbf{q}}+\mathbf{B}\dot{\mathbf{q}}+\mathbf{AS_f}(\dot{\mathbf{q}})=\mathbf{u}+\mathbf{d_n}+\widetilde{\mathbf{d}} \tag{7}$$

where $\mathbf{d_n}=[d_{n1},d_{n2}]^T$ is the nominal value of $\mathbf{d_1}=\mathbf{d}+\widetilde{\mathbf{F}}$, and $\widetilde{\mathbf{d}}=\mathbf{d_1}-\mathbf{d_n}$. Noting (4),

$$\begin{aligned} \dot{\mathbf{r}}&=\mathbf{J}\dot{\mathbf{q}}(t) \\ \ddot{\mathbf{r}}&=\mathbf{J}\ddot{\mathbf{q}}(t)+\dot{\mathbf{J}}\dot{\mathbf{q}}(t) \end{aligned} \tag{8}$$

Thus, the equation (7) can be transformed into the task coordinates as

$$\mathbf{M_t}\ddot{\mathbf{r}} + \mathbf{B_t}\dot{\mathbf{r}} + \mathbf{C_t}\dot{\mathbf{r}} + \mathbf{A_t}\mathbf{S_f}(\dot{\mathbf{q}}) = \mathbf{u_t} + \mathbf{d_t} + \widetilde{\Delta} \tag{9}$$

where

$$\mathbf{M_t} = \mathbf{J^{-T}}\mathbf{M}\mathbf{J^{-1}},\ \mathbf{B_t} = \mathbf{J^{-T}}\mathbf{B}\mathbf{J^{-1}},\ \mathbf{C_t} = -\mathbf{J^{-T}}\mathbf{M}\mathbf{J^{-1}}\dot{\mathbf{J}}\mathbf{J^{-1}},$$
$$\mathbf{A_t} = \mathbf{J^{-T}}\mathbf{A},\ \mathbf{d_t} = \mathbf{J^{-T}}\mathbf{d_n},\ \mathbf{u_t} = \mathbf{J^{-T}}\mathbf{u},\ \widetilde{\Delta} = \mathbf{J^{-T}}\widetilde{\mathbf{d}} \tag{10}$$

It is well known that equation (9) has several properties [14]: (**P1**) $\mathbf{M_t}$ is a symmetric positive definite (s.p.d.) matrix with $\mu_1\mathbf{I} \le \mathbf{M_t} \le \mu_2\mathbf{I}$ where μ_1 and μ_2 are two positive scalars; (**P2**) The matrix $\mathbf{N_t} = \dot{\mathbf{M}}_\mathbf{t} - 2\mathbf{C_t}$ is a skew-symmetric matrix. In other words, $\mathbf{s^T N_t s} = 0, \forall \mathbf{s}$; (**P3**) $\mathbf{M_t}$, $\mathbf{B_t}$, $\mathbf{C_t}$, $\mathbf{A_t}$, $\mathbf{d_t}$ and $\mathbf{u_t}$ in (9) can be linearly parameterized by a set of unknown parameters defined as $\theta = [\theta_1, ..., \theta_8]^T = [M_1, M_2, B_1, B_2, A_1, A_2, d_{n1}, d_{n2}]^T$.

In general, θ cannot be known exactly. For example, the payload of the biaxial gantry depends on tasks. However, the extent of parametric uncertainties can be predicted. Therefore, the following practical assumption can be made.

Assumption 1: The extent of parametric uncertainties and uncertain nonlinearities is known. More precisely,

$$\begin{aligned} &\theta \in \Omega_\theta \triangleq \{\theta :\ \theta_{min} \le \theta \le \theta_{max}\} \\ &\widetilde{\Delta} \in \Omega_\Delta \triangleq \left\{\widetilde{\Delta} :\ ||\widetilde{\Delta}|| \le \delta_\Delta\right\} \end{aligned} \tag{11}$$

where $\theta_{min} = [\theta_{1min}, ..., \theta_{8min}]^T$, and $\theta_{max} = [\theta_{1max}, ..., \theta_{8max}]^T$ are known constant vectors and δ_Δ is a known function.

The control objective is to synthesize a control input $\mathbf{u_t}$ such that $\mathbf{q} = [x, y]^T$ tracks a desired contour $\mathbf{q_d}(t) = [x_d, y_d]^T$ which is assumed to be at-least second-order differentiable. In the proposed task coordinate system, such an objective is achieved by simply regulating r_f to zero and letting r_g follow the desired trajectory of $r_{gd}(t) = r_g(x_d(t), y_d(t))$.

III. Discontinuous Projection

Let $\widehat{\theta}$ denote the estimate of θ and $\widetilde{\theta}$ the estimation error (i.e., $\widetilde{\theta} = \widehat{\theta} - \theta$). In view of (11), the following adaptation law with discontinuous projection modification can be used

$$\dot{\widehat{\theta}} = Proj_{\widehat{\theta}}(\Gamma\tau) \tag{12}$$

where $\Gamma > 0$ is a diagonal matrix, τ is an adaptation function to be synthesized later. The projection mapping $Proj_{\widehat{\theta}}(\bullet) = [Proj_{\widehat{\theta}_1}(\bullet_1), ..., Proj_{\widehat{\theta}_8}(\bullet_8)]^T$ is defined in [16] as

$$Proj_{\widehat{\theta}_i}(\bullet_i) = \begin{cases} 0 & if\ \widehat{\theta}_i = \theta_{imax}\ and\ \bullet_i > 0 \\ 0 & if\ \widehat{\theta}_i = \theta_{imin}\ and\ \bullet_i < 0 \\ \bullet_i & otherwise \end{cases} \tag{13}$$

It can be shown that for any adaptation function τ, the projection mapping used in (13) guarantees

$$(\mathbf{P4}) \qquad \widehat{\theta} \in \Omega_\theta \triangleq \left\{\widehat{\theta} : \theta_{imin} \le \widehat{\theta} \le \theta_{imax}\right\} \tag{14}$$

$$(\mathbf{P5}) \qquad \widetilde{\theta}^T(\Gamma^{-1}Proj_{\widehat{\theta}}(\Gamma\tau) - \tau) \le 0,\ \forall\tau \tag{15}$$

IV. Adaptive Robust Control (ARC) Law

Define a switching-function-like quantity as

$$\mathbf{s} = \dot{\mathbf{e}} + \Lambda\mathbf{e} = \dot{\mathbf{r}} - \dot{\mathbf{r}}_{\mathbf{eq}},\ \dot{\mathbf{r}}_{\mathbf{eq}} \triangleq \dot{\mathbf{r}}_\mathbf{d} - \Lambda\mathbf{e} \tag{16}$$

where $\mathbf{e} = \mathbf{r(t)} - \mathbf{r_d(t)}$ is the output tracking error, and $\Lambda > 0$ is a constant diagonal matrix. Define a positive semi-definite (p.s.d.) function

$$V(t) = \tfrac{1}{2}\mathbf{s^T}\mathbf{M_t}(\mathbf{r})\mathbf{s} \tag{17}$$

Differentiating V yields

$$\dot{V}(t) = \mathbf{s^T}[\mathbf{u_t} - \mathbf{M_t}\ddot{\mathbf{r}}_\mathbf{eq} - \mathbf{B_t}\dot{\mathbf{r}} - \mathbf{C_t}\dot{\mathbf{r}}_\mathbf{eq} - \mathbf{A_t}\mathbf{S_f}(\dot{\mathbf{q}}) + \mathbf{d_t} + \widetilde{\Delta}] \tag{18}$$

where $\ddot{\mathbf{r}}_\mathbf{eq} \triangleq \ddot{\mathbf{r}}_\mathbf{d} - \Lambda\dot{\mathbf{e}}$, and (P2) is used to eliminate the term $\frac{1}{2}\mathbf{s^T}\dot{\mathbf{M}}_\mathbf{t}(\mathbf{r})\mathbf{s}$. Furthermore, since it follows from (P3) that

$$\mathbf{M_t}\ddot{\mathbf{r}}_\mathbf{eq} + \mathbf{B_t}\dot{\mathbf{r}} + \mathbf{C_t}\dot{\mathbf{r}}_\mathbf{eq} + \mathbf{A_t}\mathbf{S_f}(\dot{\mathbf{q}}) - \mathbf{d_t} = -\Psi(\mathbf{r}, \dot{\mathbf{r}}, \dot{\mathbf{r}}_\mathbf{eq}, \ddot{\mathbf{r}}_\mathbf{eq})\theta \tag{19}$$

where $\Psi(\mathbf{r}, \dot{\mathbf{r}}, \dot{\mathbf{r}}_\mathbf{eq}, \ddot{\mathbf{r}}_\mathbf{eq})$ is a 2×8 matrix of known functions, known as the *regressor*. Equation (18) can be rewritten as

$$\dot{V}(t) = \mathbf{s^T}[\mathbf{u_t} + \Psi(\mathbf{r}, \dot{\mathbf{r}}, \dot{\mathbf{r}}_\mathbf{eq}, \ddot{\mathbf{r}}_\mathbf{eq})\theta + \widetilde{\Delta}] \tag{20}$$

Noting the structure of (20), the following ARC law is proposed:

$$\mathbf{u_t} = \mathbf{u_a} + \mathbf{u_s},\ \mathbf{u_a} = -\Psi(\mathbf{r}, \dot{\mathbf{r}}, \dot{\mathbf{r}}_\mathbf{eq}, \ddot{\mathbf{r}}_\mathbf{eq})\widehat{\theta} \tag{21}$$

where $\mathbf{u_a}$ is the adjustable model compensation needed for achieving perfect tracking, and $\mathbf{u_s}$ is a robust control law to be synthesized later. Substituting (21) into (20), and then simplifying the resulting expression leads to

$$\dot{V}(t) = \mathbf{s^T}[\mathbf{u_s} - \Psi(\mathbf{r}, \dot{\mathbf{r}}, \dot{\mathbf{r}}_\mathbf{eq}, \ddot{\mathbf{r}}_\mathbf{eq})\widetilde{\theta} + \widetilde{\Delta}] \tag{22}$$

The robust control function $\mathbf{u_s}$ consists of two terms:

$$\mathbf{u_s} = \mathbf{u_{s1}} + \mathbf{u_{s2}},\ \mathbf{u_{s1}} = -\mathbf{K}\mathbf{s} \tag{23}$$

where $\mathbf{u_{s1}}$ is used to stabilize the nominal system, and it is a simple proportional feedback with $\mathbf{K}$ being a symmetric positive definite matrix in this case, and $\mathbf{u_{s2}}$ is a robust feedback used to attenuate the effect of model uncertainties. Noting Assumption 1 and (P4), there exists a $\mathbf{u_{s2}}$ such that the following two conditions are satisfied

$$\begin{aligned} i \quad & \mathbf{s^T}\left\{\mathbf{u_{s2}} - \Psi(\mathbf{r}, \dot{\mathbf{r}}, \dot{\mathbf{r}}_\mathbf{eq}, \ddot{\mathbf{r}}_\mathbf{eq})\widetilde{\theta} + \widetilde{\Delta}\right\} \le \quad \eta \\ ii \quad & \mathbf{s^T}\mathbf{u_{s2}} \le \mathbf{0} \end{aligned} \tag{24}$$

where η is a design parameter that can be arbitrarily small. One smooth example of $\mathbf{u_{s2}}$ satisfying (24) is given by $\mathbf{u_{s2}} = -\frac{1}{4\eta}H^2\mathbf{s}$, where H is a smooth function satisfying $H \ge ||\theta_\mathbf{M}||||\Psi(\mathbf{r}, \dot{\mathbf{r}}, \dot{\mathbf{r}}_\mathbf{eq}, \ddot{\mathbf{r}}_\mathbf{eq})|| + \delta_\Delta$, and $\theta_M = \theta_{max} - \theta_{min}$.

Theorem 1: Suppose the adaptation function in (12) is chosen as

$$\tau = \Psi^\mathbf{T}(\mathbf{r}, \dot{\mathbf{r}}, \dot{\mathbf{r}}_\mathbf{eq}, \ddot{\mathbf{r}}_\mathbf{eq})\mathbf{s} \tag{25}$$

Then, the ARC control law (21) guarantees that:

A. In general, all signals are bounded. Furthermore, the positive semi-definite function $V(t)$ defined by (17) is bounded above by

$$V(t) \le exp(-\lambda t)V(0) + \tfrac{\eta}{\lambda}[1 - exp(-\lambda t)] \tag{26}$$

where $\lambda = 2\sigma_{min}(\mathbf{K})/\mu_2$, and $\sigma_{min}(\cdot)$ denotes the minimum eigenvalue of a matrix. Note that $\sigma_{min}(\mathbf{K})$ is real and positive since $\mathbf{K}$ is symmetric positive definite.

B. Suppose there exist parametric uncertainties only after a finite time t_0, i.e., $\widetilde{\Delta} = 0$, $\forall t \geq t_0$. Then, in addition to result A, zero final tracking error is also achieved, i.e, $\mathbf{e} \to 0$ and $\mathbf{s} \to 0$ as $t \to \infty$.

Proof: From of (P1), we have

$$\tfrac{1}{2}\mu_1||\mathbf{s}||^2 \leq V \leq \tfrac{1}{2}\mu_2||\mathbf{s}||^2 \tag{27}$$

From (22), (23), condition i of (24) and (27), it follows that

$$\begin{aligned} \dot{V}(t) &= -\mathbf{s^T K s} + \mathbf{s^T}[\mathbf{u_{s2}} - \Psi(\mathbf{r}, \dot{\mathbf{r}}, \dot{\mathbf{r}}_{\mathbf{eq}}, \ddot{\mathbf{r}}_{\mathbf{eq}})\widetilde{\theta} + \widetilde{\Delta}] \\ &\leq -\sigma_{min}(\mathbf{K})||\mathbf{s}||^2 + \eta = -\lambda V + \eta \end{aligned} \tag{28}$$

which leads to (26) and thus proves result *A* of Theorem 1. Now consider the situation in *B* of Theorem 1, i.e., $\widetilde{\Delta} = 0$, $\forall t \geq t_0$. Choose a positive definite function $V_\theta(t)$ as

$$V_\theta(t) = V(t) + \tfrac{1}{2}\widetilde{\theta}^T\Gamma^{-1}\widetilde{\theta} \tag{29}$$

From (28), condition ii of (24) and (P5), it follows that

$$\dot{V}_\theta(t) \leq -\mathbf{s^T K s} - \mathbf{s^T}\Psi(\mathbf{r}, \dot{\mathbf{r}}, \dot{\mathbf{r}}_{\mathbf{eq}}, \ddot{\mathbf{r}}_{\mathbf{eq}})\widetilde{\theta} + \widetilde{\theta}^{\mathbf{T}}\Gamma^{-1}\dot{\widehat{\theta}} \leq -\mathbf{s^T K s} \tag{30}$$

which shows that $\mathbf{s} \in L_2 \cap L_\infty$. It is easy to check that $\dot{\mathbf{s}}$ is bounded. So, $\mathbf{s}$ is uniformly continuous. By Barbalat's lemma, $\mathbf{s} \to \mathbf{0}$ as $\mathbf{t} \to \infty$. ■

V. Experimental Setup and Results

A. Experiment setup

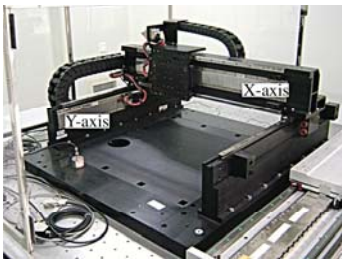

Fig. 2. A biaxial linear motor driven gantry system

To test the proposed controllers' effectiveness and study contour-following motion control of the biaxial gantry system, a biaxial Anorad gantry from Rockwell Automation is set up as a test-bed. As shown in Figure 2, the two axes of the gantry are mounted orthogonally with X-axis on top of Y-axis. The position sensors of the gantry are two linear encoders with a resolution of $0.5\mu m$ after quadrature. The velocity signal is obtained by the difference of two consecutive position measurements. Standard least-square identification is performed to obtain the parameters of the biaxial gantry and it is found that nominal values of the gantry system parameters without loads are $M_1 = 0.12\ V/m \cdot s^2$, $M_2 = 0.5\ V/m \cdot s^2$, $B_1 = 0.45\ V/m \cdot s$, $B_2 = 0.65\ V/m \cdot s$, $A_1 = 0.1\ V$, $A_2 = 0.15\ V$The bounds of the parametric variations are chosen as $\theta_{min} = [0.06, 0.45, 0.35, 0.5, 0.05, 0.08, -0.5, -1]^T$ and $\theta_{max} = [0.25, 0.6, 0.55, 0.8, 0.15, 0.25, 0.5, 1]^T$

B. Experimental Results

The control algorithms are implemented using a dSPACE DS1103 controller board. The controller executes programs at a sampling period $T_s = 0.2ms$, which results in a velocity measurement resolution of $0.0025m/sec$. To test the effectiveness of the proposed task coordinate frame, the following two task coordinate frames with ARC algorithms are compared:

C1: The traditional task coordinate frame presented in [11], [12] shown in Figure 3. Let x and y denote the horizontal and the vertical axes of a biaxial gantry system. P_d and P_a denote the position of the reference command and the actual position of the system at any time instant respectively. At the point P_d, the desired contour possesses a set of tangential and normal directions such that the contouring error can be approximated by the distance from P_a to the tangential line in the normal direction. The physical (x, y) coordinates can be transformed into the task $(\varepsilon_c, \varepsilon_t)$ coordinates by a linear time-varying transformation

$$\varepsilon = \mathbf{T}\mathbf{e} \tag{31}$$

where $\varepsilon = [\varepsilon_c, \varepsilon_t]^T$; $\mathbf{e} = [e_x, e_y]^T$, e_x and e_y denote the axial tracking errors of x and y axes, i.e. $e_x = x - x_d$, $e_y = y - y_d$, α denotes the angle between the tangential line to the horizontal X-axis, and the time-varying transformation matrix depends on the reference trajectories for the desired contour only and is given by

$$\mathbf{T} = \begin{bmatrix} -sin\alpha & cos\alpha \\ cos\alpha & sin\alpha \end{bmatrix} \tag{32}$$

The matrix $\mathbf{T}$ is always unitary for all values of α, i.e., $\mathbf{T^T} = \mathbf{T}$ and $\mathbf{T^{-1}} = \mathbf{T}$. In this model, if the axial tracking errors are comparatively small to the curvature of the desired contour, then it yields a good approximation of the contouring error.

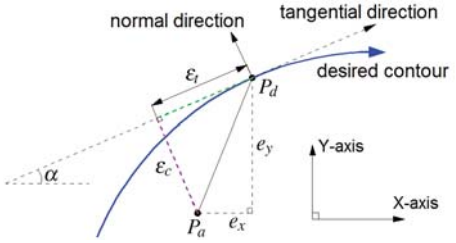

Fig. 3. An approximate contouring error model

C2: The proposed task coordinate frame in this paper.

In C1 and C2, the smooth functions $S_f(\dot{x})$ and $S_f(\dot{y})$ are chosen as $\frac{2}{\pi}arctan(9000\dot{x})$ and $\frac{2}{\pi}arctan(9000\dot{y})$. Λ is chosen as: $\Lambda = diag[100, 30]$. $\mathbf{u_{s2}}$ in (23) is theoretically given in section IV. In implementation, a large enough constant feedback gain is used instead to simplify the resulting control law as done in [12]–[14]. With this simplification, the feedback gain in (23) is chosen as: $\mathbf{K} = diag[100, 60]$. The adaptation rates are set as $\Gamma = diag[10, 10, 10, 10, 1, 1, 10000, 10000]$. The initial parameter estimates are chosen as: $\widehat{\theta}(0) = [0.12, 0.5, 0.45, 0.65, 0.1, 0.15, 0, 0]^T$. Note that with these control gains, C1 is exactly same as that in [12].

The following test sets are performed:

Set1 : To test the nominal contouring performance of the controllers, experiments are run without payload;

Set2 : A large step disturbance (a simulated 0.8 V electrical signal) is added to the input of Y axis at t=10.4 sec and removed at t=13.4 sec to test the performance robustness of each controller to disturbance.

Set3 : To test the performance robustness of the algorithms to parameter variations, a 5 kg payload is mounted on the gantry;

1) Small-curvature elliptical contouring: The gantry is first commanded to track a small-curvature contour given by

$$\mathbf{q_d} = \begin{bmatrix} x_d(t) \\ y_d(t) \end{bmatrix} = \begin{bmatrix} 0.2sin(3t) \\ -0.1cos(3t)+0.1 \end{bmatrix} \quad (33)$$

which has an angular velocity of $w = 3rad/sec$.

2) Large-curvature elliptical contouring: The gantry is also commanded to track a large-curvature contour given by

$$\mathbf{q_d} = \begin{bmatrix} x_d(t) \\ y_d(t) \end{bmatrix} = \begin{bmatrix} 0.2sin(4t) \\ -0.02cos(4t)+0.02 \end{bmatrix} \quad (34)$$

which has an angular velocity of $w = 4rad/sec$.

TABLE I

CONTOURING RESULTS

Small-curvature contouring results				
	$\|\|\varepsilon_c\|\|_{rms}(\mu m)$	$\varepsilon_{cM}(\mu m)$	$\|\|u_x\|\|_{rms}(V)$	$\|\|u_y\|\|_{rms}(V)$
C1 (Set1)	3.00	12.01	0.36	0.47
C2 (Set1)	2.39	8.76	0.37	0.47
C1 (Set2)	3.37	38.25	0.36	0.62
C2 (Set2)	2.91	38.16	0.37	0.62
C1 (Set3)	3.27	14.94	0.41	0.50
C2 (Set3)	2.42	9.66	0.41	0.50
Large-curvature contouring results				
	$\|\|\varepsilon_c\|\|_{rms}(\mu m)$	$\varepsilon_{cM}(\mu m)$	$\|\|u_x\|\|_{rms}(V)$	$\|\|u_y\|\|_{rms}(V)$
C1 (Set1)	2.59	12.15	0.46	0.27
C2 (Set1)	1.55	6.87	0.46	0.30
C1 (Set2)	2.99	36.39	0.46	0.46
C2 (Set2)	1.97	36.23	0.47	0.47
C1 (Set3)	2.68	12.56	0.57	0.28
C2 (Set3)	1.63	6.92	0.56	0.31

The experimental results of small-curvature and large-curvature contouring in terms of all performance indexes after running the gantry for several periods are given in Table I, in which the following performance indexes are used to measure the quality of each algorithm: (i) $||\varepsilon_c||_{rms} = (\frac{1}{T}\int_0^T |\varepsilon_c|^2 dt)^{1/2}$, the root-mean-square (RMS) value of the contouring error to measure average contouring performance where T is the total running time; (ii) $\varepsilon_{cM} = \max_t\{|\varepsilon_c|\}$, the maximum absolute value of the contouring error to measure transient performance; and (iii) $||u_i||_{rms} = (\frac{1}{T}\int_0^T |u_i|^2 dt)^{1/2}$, the average control input of each axis to evaluate the amount of control effort. As seen from the table, C2 performs better than C1 in terms of all indexes using almost the same amount of control efforts for every test set. Figure 4 – 9 show the results of the low-curvature and large-curvature contouring performances. In the small-curvature contouring results, the desired contour and the actual contours by C1 and C2 are partially shown in Figure 4 for Set1, which directly demonstrates that C2 achieve better contouring results than that of C1 – the contour of C2 are quite closed to the desired contour; for Set2, the contouring errors are displayed in Figure 5, it is seem that the added large disturbances do not affect the contouring performance much except the transient spikes when the sudden changes of the disturbances occur; for Set3, the contouring errors are given in Figure 6, which shows that both controllers achieve good steady-state contouring performance in spite of the change of inertia load, also verifying the performance robustness of the proposed ARC controllers to parameter variations. In the large-curvature contouring results, the contouring errors are displayed in Figure 7 for Set1, it is seem that the C2 achieves much better contouring performances than that of C1, which demonstrates that C2 can achieve excellent contouring performance even when large-curvature contouring task is required; this conclusion can also be validated by Figure 8 for Set2 and Figure 9 for Set3, in which the desired contours and the actual contours by C1 and C2 are partially shown for further comparison and demonstration. Overall, all these results demonstrate that the proposed task coordinate frame can achieve excellent contouring performance. And the proposed frame can achieve better contouring performances than that of the traditional task coordinate frame, especially under the tasks of large-curvature contouring.

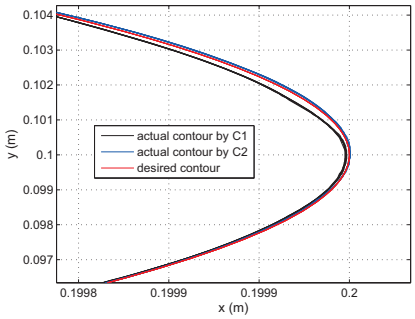

Fig. 4. Partial small-curvature contours of Set1

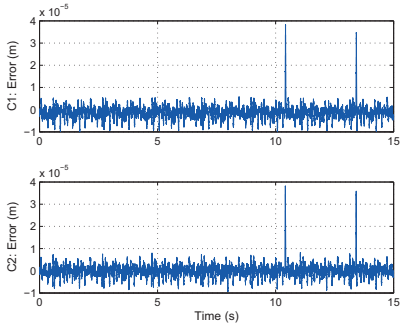

Fig. 5. Small-curvature contouring errors of Set2

VI. CONCLUSIONS

This paper proposed a global task coordinate frame (TCF) for contouring control of biaxial systems for high-speed and

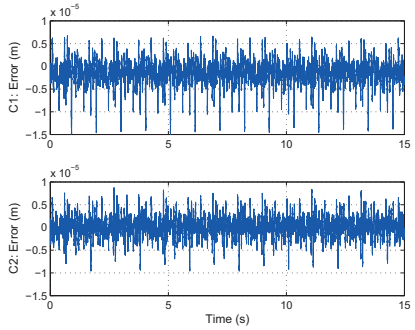

Fig. 6. Small-curvature contouring errors of Set3

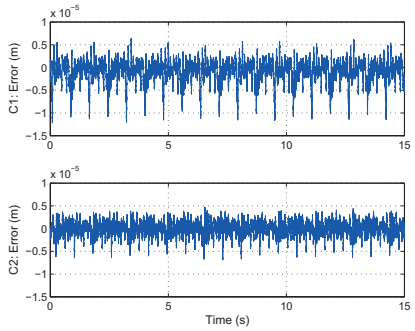

Fig. 7. Large-curvature contouring errors of Set1

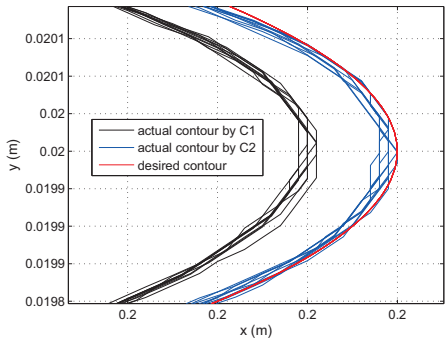

Fig. 8. Partial large-curvature contours of Set2

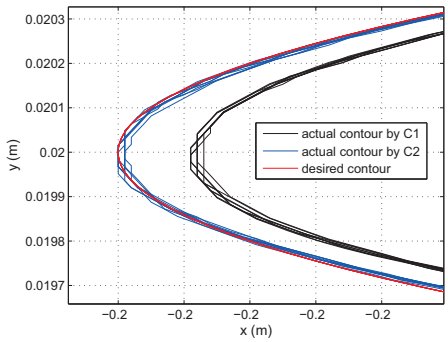

Fig. 9. Partial large-curvature contours of Set3

large-curvature contouring applications. Comparative experimental results obtained on a high-speed industrial biaxial gantry driven by linear motors were presented and verified the effectiveness and the excellent contouring performance of the proposed TCF based ARC controller for both high-speed small-curvature and large-curvature motions.

REFERENCES

[1] Y. Koren and C. C. Lo, "Variable gain cross coupling controller for contouring," *CIRP Proc.-Manufacturing Systems*, vol. 40, pp. 371–374, 1991.

[2] Y. Koren and C. C. Lo, "Advanced controllers for feed drives," *CIRP Proc.-Manufacturing Systems*, vol. 41, no. 2, pp. 689–698, 1992.

[3] S. S. Yeh and P. L. Hsu, "Theory and applications of the robust cross-coupled control design," in *Proc. American Control Conference*, 1997, pp. 791–795.

[4] Y. T. Shih, C. S. Chen, and A. C. Lee, "A novel cross-coupling control design for bi-axis motion," *Int. J. Mach. Tools Manuf.*, vol. 42, pp. 1539–1548, 2002.

[5] S.-S. Yeh and P.-L. Hsu, "Estimation of the contouring error vector for the cross-coupled control design," *IEEE/ASME Transactions on Mechatronics*, vol. 7, no. 1, March 2002.

[6] Y. Xiao and K. Y. Zhu, "Optimal synchronization control of high-precision motion systems," *IEEE Transactions on Industrial Electronics*, vol. 53, no. 4, pp. 1160–1169, Aug. 2006.

[7] K.-H. Su and M.-Y. Cheng, "Contouring accuracy improvement using cross-coupled control and position error compensator," *International J. of Machine Tools and Manufacture*, vol. 48, pp. 1444–1453, 2008.

[8] Y. Koren, "Cross-coupled biaxial computer control for manufacturing systems," *ASME J. Dynamical Systems, Measurement, and Control*, vol. 102, pp. 265–272, 1980.

[9] G. T.-C. Chiu and M. Tomizuka, "Contouring control of machine tool feed drive systems: a task coordinate frame approach," *IEEE Trans. Control System Technology*, vol. 9, pp. 130–139, Jan. 2001.

[10] M.-Y. Cheng and C.-C. Lee, "Motion controller design for contour-following tasks based on real-time contour error estimation," *IEEE Trans. on Indus. Elect.*, vol. 54, no. 3, pp. 1686–1695, June 2007.

[11] C.-L. Chen and K.-C. Lin, "Observer-based contouring controller design of a biaxial stage system subject to friction," *IEEE Transactions on Control System Technology*, vol. 16, no. 2, pp. 322–329, March 2008.

[12] C. Hu, Bin Yao, and Q. Wang, "Coordinated adaptive robust contouring controller design for an industrial biaxial precision gantry," *IEEE/ASME Transactions on Mechatronics*, 2010. (Accepted in 2009 and in press). Part of the paper was presented in 2009 IEEE/ASME Conference on Advanced Intelligent Mechatronics.

[13] C. Hu, Bin Yao, and Q. Wang, "Coordinated adaptive robust contouring control of an industrial biaxial precision gantry with cogging force compensations," *IEEE Transactions on Industrial Electronics*, Vol. 57, no. 5, pp. 1746–1754, May 2010. Part of the paper was presented in 2009 ASME Conference on Dynamic Systems and Control.

[14] C. Hu, Bin Yao, and Q. Wang, "Integrated Direct/Indirect Adaptive Robust Contouring Control of a Biaxial Gantry with Accurate Parameter Estimations," *Automatica*, Vol. 46, no. 4, pp. 701–7, April 2010.

[15] S.-L. Chen and K.-C. Wu, "Contouring control of smooth paths for multi-axis systems based on equivalent errors," *IEEE Transactions on Control System Technology*, vol. 15, no. 6, pp. 1151–1158, 2007.

[16] B. Yao, "High performance adaptive robust control of nonlinear systems: a general framework and new schemes," in *IEEE Conference on Decision and Control*, 1997, pp. 2489–2494.

[17] B. Yao and M. Tomizuka, "Adaptive robust control of SISO nonlinear systems in a semi-strict feedback form," *Automatica*, vol. 33, no. 5, pp. 893–900, 1997.